Effects of Varying Arc Angles and Poles Numbers on Force Characteristics of Switched Reluctance (SR) Actuator

I.Yusri, M.M.Ghazaly*, M.F.Rahmat, S.H.Chong, R.Ranom, Z.Abdullah, S.P.Tee, C.K.Yeo

***Abstract*— This paper presented the optimum performances of Switched Reluctance (SR) actuator based on the force characteristics. The validations were done by using Finite Element Analysis (FEM) using ANSYS Maxwell 3D software to obtain the distributions of magnetic flux for different configurations. The number of poles and the arc angles parameters are the main concerned. Initially, the number of poles is set to stator-to-rotor (S:R) = 6:4 poles ratio which is then varied by increasing the ratio. In addition, the arc angle for stator (βs) and rotor (βr) were also varied by ±2° degree for each configuration. Based on FEM analysis, the best results were achieved by the SR actuator with the parameters of S: R = 6:4 poles ratio and the arc angles, βs/βr = 30°/41°. This configurations show the highest and most stable increment of force compared to the others configuration.**

***Index Term*— Electromagnetic; Finite Element Analysis; stator and rotor pole arc; variable number of poles**

I. Introduction

Researches in the field of actuator conducted recently are more focus on the design of actuators for industrial applications. Among the actuators which are often used in research are electromagnetic actuators, electrostatic actuators and hydraulic actuators. These types of actuators have their own advantages for different applications. Table I summarize the comparisons of the actuators based on their general applications [1-6].

TABLE I
COMPARISONS OF ELECTROMAGNETIC, ELECTROSTATIC AND HYDRAULIC ACTUATOR

Actuator type	Structure	Torque	Characteristic Model
Electromagnetic	Simple	High	Nonlinear
Electrostatic	Simple	Small	Nonlinear
Hydraulic	Simple	High	Nonlinear

This research and its publication are supported by Ministry of Higher Education Malaysia **(**MOHE**)** under the Research Acculturation Collaboration Effort (RACE) grant, no.RACE/F3/TK5/FKE/F00249.

I.Yusri, M.M.Ghazaly*, S.H.Chong, R.Ranom, S.P.Tee and C.K.Yeo are with the Center for Robotics and Industrial Automation (CeRIA), Faculty of Electrical Engineering, Universiti Teknikal Malaysia Melaka, Hang Tuah Jaya, 76100 Durian Tunggal, Melaka, Malaysia (*corresponding author phone: +6065552314; e-mail: mariam@utem.edu.my).

M.F.Rahmat is with the Faculty of Electrical Engineering, Universiti Teknologi Malaysia, 81310 UTM Johor Bahru, Johor, Malaysia.

Z.Abdullah is with the Faculty of Manufacturing Engineering, Universiti Teknikal Malaysia Melaka, Hang Tuah Jaya, 76100 Durian Tunggal, Melaka, Malaysia

.

Electromagnetic actuator is one of the electric motor that converts an electrical input power to a mechanical output power. There are many researches being done that incorporate electromagnetic actuator in industrial applications. One of the strong demand was on developing the hybrid electric vehicles (HEV) [6,7]. Most of the applications which adopted Permanent Magnet (PM) actuator are trying to be replaced by Switched Reluctance (SR) actuator such as blower and high speed-pump [9,10] . These applications require high speed drive but with compact structure and lightweight which SR actuator can fulfill. Thus, this paper will discuss the design of SR actuator which incorporate these applications.

Since SR actuator is still new in the industry, most of the developed electric motor are consuming rare-earth material or permanent magnet in the structures which are relatively expensive and may cause pollution [11]. The price and the availability of this material have been recognized as the major problems for the motor productions [1].

Therefore, recent researches have focused on the development of SR actuator which uses recyclable material such as steel core and copper wire [12]. Several advantages of the SR actuators are the actuator has a simple structure, low cost, rotor robustness, high speed, and possible operation in high temperature and high rotational speed [6, 9-11]. However, there are still few disadvantages of the SR actuator; i.e.; (1) low torque-to-volume ratio; (2) low efficiency; (3) require unique inverters and 4) torque ripple [12,13].

Therefore, to overcome these problems in the SR actuator, the actuator's parameters were varied based on the original designed for high performances. Among the parameters that gave impact on the force characteristics are the stator-to-rotor poles (S:R) ratio and the arc angle of the stator (βs) and rotor (βr) [17]. These two parameters will affect the SR actuator's active regions area. The SR actuator is an actuator with parameters that is easy to diversify due to its simple structure [18]. The constructions only involves two types of materials which are the core material and the winding turn's material [19].

Therefore, in this paper a new design of SR actuator was evaluated for determining the optimize force characteristics when the stator-to-rotor poles ratio (S:R) and the arc angle of the stator (βs) and rotor (βr) are varied. The analyses were done by using ANSYS Maxwell 3D software using the Finite Element analysis (FEM) in order to verify the static force.

In section 2, this paper will be discussed the fundamentals of the SR actuator as well as the geometric construction for the design. The effect of varying the parameters will also be described further in this section. In Section 3, the FEM results and discussions for varying the actuator's parameters are discussed. The last section will conclude the chosen SR actuator configurations based on the optimized force characteristics.

II. Methodology

A. Fundamentals of electromagnetic actuator

The SR actuator operates based on Switched Reluctance Motor (SRM) principles. Figure 1 illustrates the construction of a 3-phase SRM. When the wire coils are applied with current, magnetic field will form around the wire coil and causes a flux linkage between stator and rotor. Equation 1 shows that the electromagnetic torque are proportional to the amount of excitation current [12, 18]. Higher value of current will results in stronger magnetic field. The flux linkage between these two cores will cause the rotor to rotate. The other factor that contributes to the value of torque is the position of rotor with respect to the stator poles. Figure 1 shows the basic principle of the SRM. Each coil is wounded around a single stator pole. The winding will results in the built of North (N) polarity and South (S) polarity at the stator pole which produce the motion of the SR actuator. By having 12 number of stator poles, this will results in three difference flow of magnetic flux. Each group consists of 4 stator poles which are attached to different phase of current source. At first phase, a group of 4 poles will be supplied with current. These groups will caused the rotor to the position where the stator and rotor poles will be aligned [21]. As the phase's changes, the next group of 4 poles will cause the rotor to move and the process is continued for the next phase.

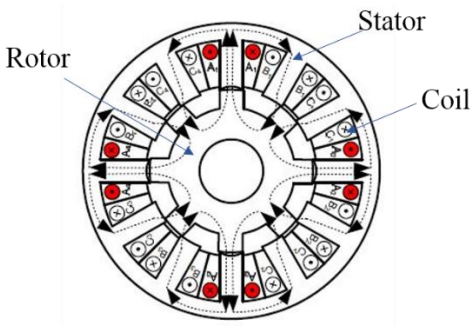

Fig. 1. Direction of flux linkage of stator-to-rotor ratio;12:8 for SRM [21]

$$Te = \frac{1}{2}.i^2.\frac{dL(\theta,i)}{d\theta} \quad (1)$$

Where,

T_e = Electromagnetic torque

i = Excitation current

$L(\theta,i)$ = Inductance dependent on the rotor position and phase current

B. Effects of the arc angle towards the distribution of magnetic flux

Based on the previous researches [19, 20], considerations on the arc angle is important to maintain proper initial self-starting force and to create a fully unaligned position for the stator and rotor poles configurations. Figure 2 shows the geometrical dimension of the arc angle for S:R = 6:4 poles ratio configuration; where βr is arc angle for rotor; βs is arc angle for stator; L_u is length for rotor unaligned position and L_{spa} is length of stator's pole respectively.

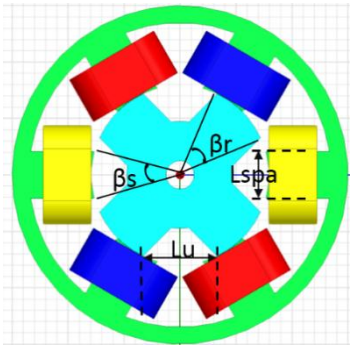

Fig. 2. Geometrical dimension of the arc angle for S:R = 6:4 poles ratio

The S:R = 6:4 design is based on the original 3-phase SRM. Based on Figure 2, the total number of stator poles is 6; where each phase has a pair of poles. Each phase will be induced with the similar excitation current, but with a phase delay. This also applies to S: R = 12:8 poles ratio configuration, where each group will contain four stator poles. In order to maintain the 3-phase system configurations, number of poles ratio was doubled from the initial parameter. In Figure 2, the similar color of poles is considered as one (1) group. The phases was assigned as describe in Table II.

TABLE II
LABELLING OF 3-PHASE SYSTEM SR ACTUATOR'S PART

Part	Label
Phase A	
Phase B	
Phase C	
Stator	
Rotor	

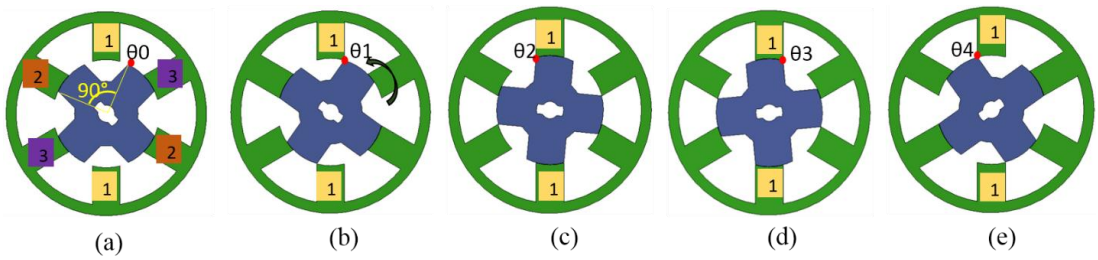

Fig. 3. Rotor position to derive the inductance profile

From literature reviews, the changes on the arc angle will directly gave affect to the size of the actuator. The flux linkage between the rotor and stator is altered as the area of the active region changes. In conventional SRM for S:R = 6:4 poles ratio, the arc angle for rotor will be slightly greater than the stator to achieve the best performances ($\beta r > \beta s$) [20, 22]. The reasons was to create a dead time inductance profile for the turn-off delay and maintain the fully unaligned position of the rotor as shown in Figure 3(a). The definitions of unaligned position are described as length of unaligned
position (L_u) is greater than the length of stator pole arc (L_{spa}); thus $L_u > L_{spa}$ [22].

The initial position of rotor is important to determine the inductance profile of the SR actuator. For configuration of S:R = 6:4 poles ratio, there are five positions that were a concerned as shown in Figure 3. Figure 4 shows the overlapping inductance profile based on the unaligned position of the rotor shown in Figure 3. In Figure 3(a), initially the rotor position is fully unaligned as θ_0. When the first phase started to excite the current, the rotor rotates and touched the edge of the stator core at θ_1. This is where the inductance value rises gradually and then reached dead time when both stator and rotor are aligned (L_a); i.e from θ_2 to θ_3. To maintain the continuous rotations for the 3-phase system, the second phase will excite the current during position of θ_2. Together with the combinations momentum of rotations, the rotor is rotated in one direction according to the arrangement of phases, i.e. configuration in Figure 3 was assigned to rotate in anticlockwise direction. Therefore, it is important to define the suitable arc angle for stator and rotor to accommodate with the SR actuator inductance profile.

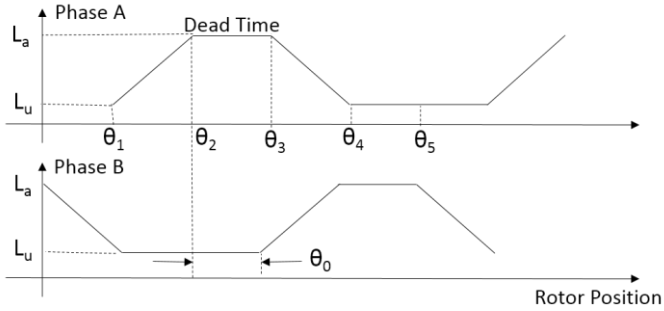

Fig. 4. Typical overlapping inductance profile

C. *Area of the active region for flux linkage.*

The distributions of magnetic flux are closely related to the area of the active region. When the same dimension geometry of the stator and rotor is maintained, these areas are mostly affected by number of poles and arc angle. Increasing the number of poles will cause this area to reduce in size and the magnetic flux path will become narrower. Figure 5 shows the details of the active region areas. The red colored surface is the area of the active region which is linked the rotor and stator core.

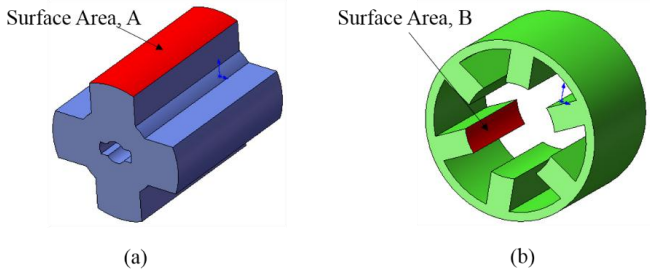

Fig. 5. Area of the active region for (a) rotor and (b) stator

D. *Construction design of switched reluctance (SR) actuator*

For the geometric optimization, the analyses were made by varying one of the initial parameters, while the other parameters are fixed. The parameters that were varied are the stator-to-rotor poles (S:R) ratio and the arc angle of the stator (βs) and rotor (βr). Figure 6 and 7 shows the actuators structure for two types of poles ratio, i.e. S:R = 6:4 and 12:8 respectively. The number of poles is limited to these two configurations due to the space constraint for winding purposes. One hundred (100) of winding turns must be fixed into each pole without contact between adjacent winding during the developing of the prototype. Table III shows the initial parameters for both configurations. There were used same materials which is Low Carbon Steel (Steel 1008) to maintain the same characteristic. The effect of hysteresis and eddy loss of the materials is neglected during the simulations.

Initially, the design was set accordance to the initial parameters stated in Table III. The parameters that are a concerned in this analysis are the number of poles and arc angle. Based on the initial values, the arc angles for stator and rotor were varied with an interval of ±2° as shown in Table IV, in order to optimize the force characteristics. For S:R = 6:4 poles ratio, the initial arc angle is $\beta s/\ \beta r$ =41°/30°. Meanwhile, for the S:R = 12:8 poles ratio configuration, the initial parameters for arc angle is set to $\beta s/\ \beta r$ =15°/20° [25]. Figure 8 shows the geometric views for S:R poles ratio configuration

where D_o is the outer diameter of the stator; D_i is the inner diameter of the stator where measured from two tips of stator's pole and H is the height for both stator and rotor core respectively.

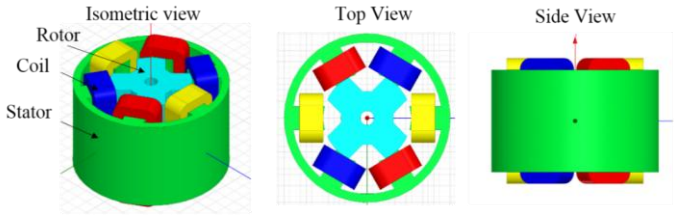

Figure 6 Structure of S:R = 6:4 poles ratio actuator

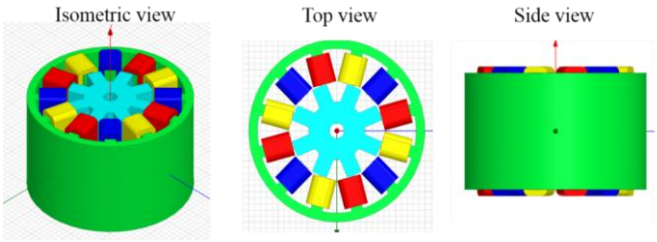

Fig. 7. Structure of S:R = 12:8 poles ratio actuator

TABLE III
INITIAL PARAMETER SR ACTUATORS CONFIGURATION

Parameters	Value	
	S:R=6:4	S:R=12:8
Stator outer diameter, D_o	60 mm	60 mm
Stator inner diameter, D_i	31.6 mm	31.6 mm
Air gap thickness, G	0.2 mm	0.2 mm
Winding number	100 Turns	100 Turns
Stator and rotor height, H	36 mm	36 mm
Stator arc angle, β_s	30°	15°
Rotor arc angle, β_r	41°	20°

TABLE IV
PARAMETER FOR VARYING ARC ANGLE

Poles configuration	Value	
	Stator arc angle, βs (°)	Rotor arc angle, βr (°)
S:R = 6:4	28	39
	29	40
	30	41
	31	42
	32	43
S:R = 12:8	13	18
	14	19
	15	20
	16	21
	17	22

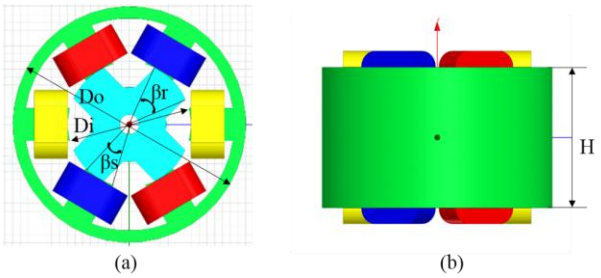

Fig. 8. Geometry structure of S:R = 6:4 poles configuration (a) top and (b) side view

III. FINITE ELEMENT ANALYSIS (FEM) RESULTS AND DISCUSSION

This section discussed, analyze and validates the force characteristics results based on FEM analysis which includes the comparisons of force characteristics when; (i) varying the number of stator-to-rotor ratio poles, and (ii) varying the arc angles for stator and rotor. Since the analysis is performed using single phase, thus the analysis results reflect the static force of the actuator. There is no motion configured during the analysis.

A. Force characteristic for different number of poles configuration

The number of poles ratio is one of the parameter that will affect the force characteristics of the SR actuator. The flux linkage that connects the stator to rotor is limited due to the decreasing of the area of active region, as discussed previously in Section 2. The smaller the area, the lower the resulting forces. In this section, two pole ratios were evaluated; i.e. S:R=6:4 and 12:8. Based on Table III, the initial parameters for both ratios were fixed accordingly, in order to evaluate the force characteristics. In addition, the excitation current used for the actuator were varied between the range of 0 A to 2.0 A with interval of 0.5 A. Based on Figure 9, it can be depicted that the S:R = 6:4 poles ratio gave a higher force compared to the S:R = 12:8 poles ratio with 1.697 N force difference when the excitation current is set to 2 A. It shows that the area of active region plays an important role in the production of the force.

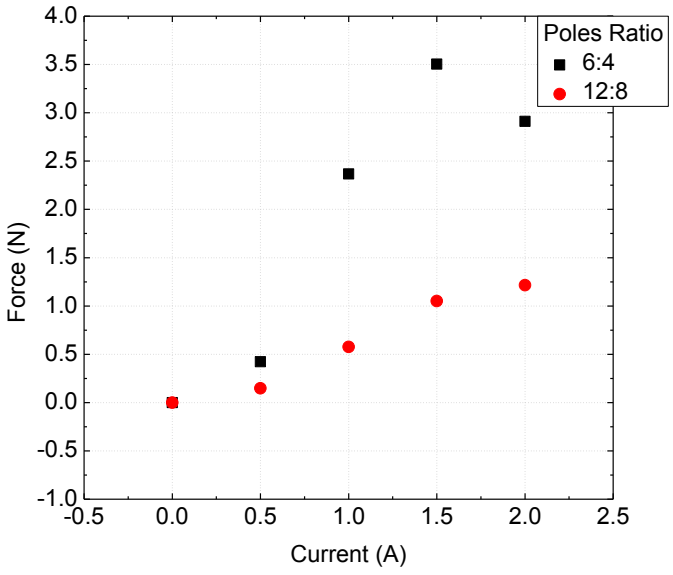

Fig. 9. FEM result of force characteristic for S:R = 6:4 and 12:8 poles ratio when air gap thickness is 0.2 mm

Figure 10 shows the distribution of magnetic flux was different for these two ratios. Due to the large space difference for the S:R = 6:4 poles ratio, more flux linkage will accumulate between the stator and the rotor in compared to the S:R = 12:8 poles ratio type ratio. Based on Table V and Figure 11, the area of active region (A and B) for the S:R = 6:4 poles ratio is twice larger than compared to S:R = 12:8 poles ratio. Since the magnetic flux linkage flows throughout the area, it gave a significant different to the force formation. Figure 11 illustrates the area of active region for both types of poles ratio configurations.

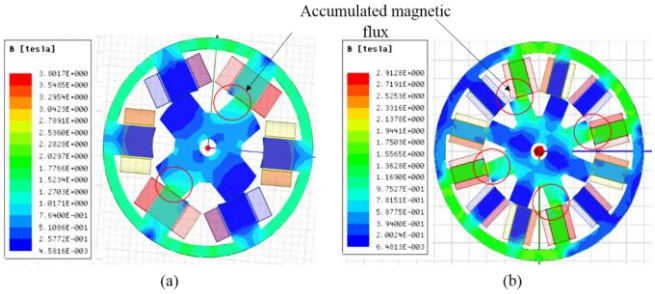

Fig. 10. Distribution of magnetic flux for S:R poles ratio (a) 6:4 and (b) 12:8

TABLE V
AREA OF ACTIVE REGION AT STATOR AND ROTOR POLES

S:R ratio poles	Surface	Area (mm^2)
6:4	A1	407.42
	B1	299.64
12:8	A2	199.24
	B2	149.85

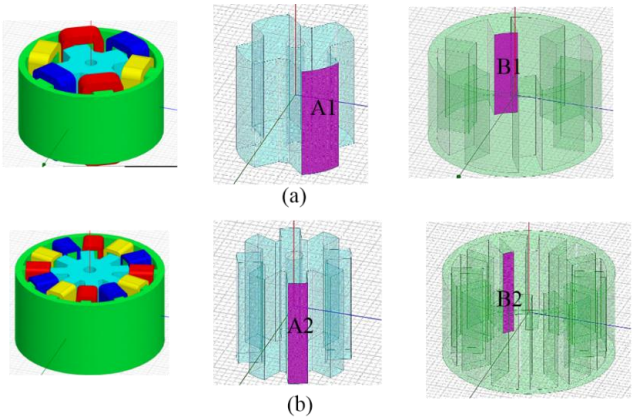

Fig. 11. Area of active region for S:R poles ratio (a) 6:4 and (b) 12:8

B. Force characteristic for different arc angle in S:R = 6:4 poles ratio

In this section the effect of arc angles to the force characteristics are evaluated for the S:R=6:4 poles ratio, with 0.2 mm air gap thickness. Figure 12 shows the FEM analysis results obtained from S:R = 6:4 poles ratio configuration for varied arc angle, as shown in Table IV. It can be depicted that the highest force is obtained when βs/βr = 28°/39° while the lowest force is generated by βs/βr = 31°/42°.

Even though the arc angle βs/βr = 28°/39° is the smallest configurations, it manages to generate the highest force. But, the core's volume is sufficient enough for the excitation current which is less than 1 A. The current was limited to 1 A for the arc angle βs/βr = 28°/39° and 29°/40°. Any further increase of current will cause a sudden drop of force; namely called the saturation effect. This effect is due to the core needs a higher volume to accommodate the increase of magnetic flux. In order to avoid saturation effect, the volume of the core for both stator and rotor were set to the maximum value. This can be done by increases the arc angle of the stator (βs) and rotor (βr). The consequences from increasing the arc angle to βs/βr = 30°/41°, 31°/42° and 32°/43° were that the saturation effect occurs at a higher applied excitation current, 1.5A. Increasing the arc angle will directly affect the total volume of the core. Thus, this improves the core's capability in order to withstand high magnetic flux. It can be depicted from Figure 12 that as the arc angle increases, the force characteristic are less towards saturation level. However, it still yet encounters saturation effect when the excitation current beyond 1.5A but is tolerable compared to the other arc angle configurations.

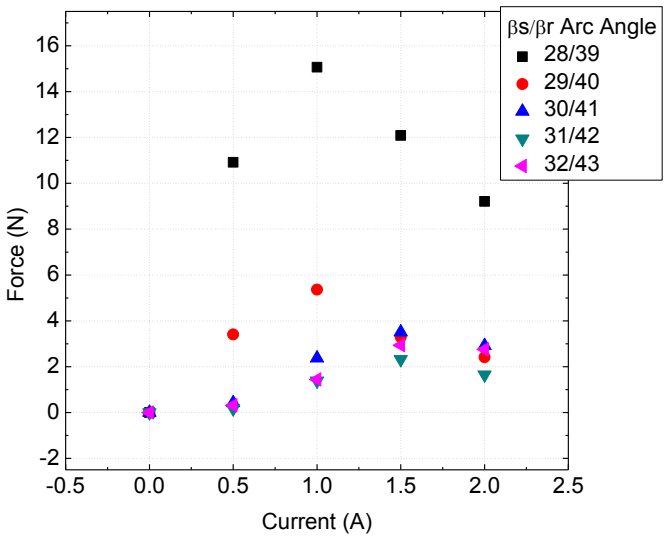

Fig. 12. FEM result of force characteristic for varying arc angle for S:R = 6:4 poles ratio with air gap thickness is 0.2 mm

C. *Force characteristic for different arc angle in S:R = 12:8 poles ratio*

Similarly, in this section the effect of arc angles to the force characteristics are evaluated for the S:R=12:8 poles ratio, with 0.2mm air gap thickness. Based on Figure 13, at the maximum excitation current (2 A), the highest force obtained is 1.784 N with the arc angle βs/βr = 16°/21°. The greater the arc angle value, the higher the value of the resulting force. However, for βs/βr = 13°/18°, 14°/19° and 13°/18° poles ratio configurations, the saturation effect occurs when the excitation current reached 1.5A. Therefore, 1.5A is established as the current limitation for that particular arc angle and poles ratio configuration. The saturation effect occurs later compare to S:R = 6:4 poles ratio configuration due to the doubled number of poles ratio. The magnetic flux is distributed thoroughly the stator and rotor during each phase since it has two pairs of active's pole. This will cause more magnetic flux linkage between the cores.

Based on Figure 12, there are two arc angle configurations that have not experience saturation effect which is βs/βr = 15°/20° and βs/βr = 17°/22°, respectively. Both resultant torques increased with the increase of excitation current. The magnetic flux is well distributed for each pair of the pole, with larger area of the active region. Based on the result, βs/βr = 15°/20° arc angle configuration has been chosen as the most stable configuration due it's high outputted force for S:R=12:8 poles ratio.

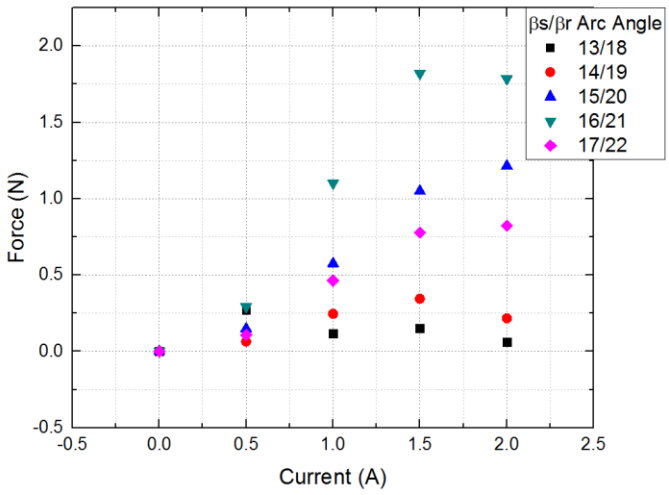

Fig. 13. FEM result of force characteristic for varying arc angle for S:R = 12:8 poles ratio when air gap thickness is 0.2 mm

D. *Optimized geometric design based on FEM analysis*

The analysis results for the force characteristics of both poles ratios configurations are almost similar where the force increases with the increased of the excitation current. However, the selected configuration is based on the highest force and smallest standard deviation. In this research, the selected optimize design was S:R = 6:4 poles ratio with the arc angle βs/βr = 30°/41°. Even though the value of force is moderate which is 2.912 N compared to the other arc angle configurations, the optimize design have a stable force which helps to control the torque ripple in the future design.

IV. Conclusions

The force characteristics of varying pole numbers and the arc angles have been presented in this paper. Simulation results of FEM have shown interesting distribution of magnetic flux and the force characteristic of the SR actuator configurations. Table VI shows the summary of the optimize force characteristic for each S:R poles ratio configurations with their suitable arc angles. The optimized parameter will next be used for future fabrication and experimental works. From Table VI, the optimized SR actuator design is chosen as S:R=6:4 pole ratio. This paper has shown that the number of pole was not the only parameters that affect the force characteristics but the arc angle played an important role. Despite small changes in the arc angle; i.e. 1°, the resulting force gave significant difference. A stable and high-value force characteristics are obtained from S:R = 6:4 pole ratio configuration and generates 2.912 N force once the maximum current excitation is 2 A.

TABLE VI
FORCE CHARACTERISTIC WHEN THE EXCITATION CURRENT IS 2A

No	Varying Parameter		Value	
1	S:R poles ratio		6:4	12:8
2	Arc angle	Stator , βs	30°	13°
		Rotor, βr	41°	18°
	Maximum Force (N)		2.912	1.784

V. Acknowledgment

Authors are grateful to Universiti Teknikal Malaysia Melaka (UTeM) and UTeM Zamalah Scheme for supporting the research. This research and its publication are supported by Research Acculturation Collaboration Effort (RACE) grant, no.RACE/F3/TK5/FKE/F00249 and Center for Research and Innovation Management (CRIM).

References

[1] M. Takeno, S. S. Member, Y. Takano, A. Chiba, N. Hoshi, M. Takemoto, S. Ogasawara, and T. Imakawa, "Torque Density and Efficiency Improvements of a Switched Reluctance Motor Without Rare-Earth Material for Hybrid Vehicles," *IEEE Trans. Ind. Appl.*, vol. 47, no. 3, pp. 1240–1246, 2011.

[2] S. Salleh, M. F. Rahmat, S. M. Othman, and H. Z. Abidin, "Application of draw wire sensor in the tracking control of an electro hydraulic actuator system," *J. Teknol.*, vol. 73, no. 6, pp. 51–57, 2015.

[3] E. Pengwang, K. Rabenorosoa, M. Rakotondrabe, and N. Andreff, "Characterization and micro-assembly of electrostatic actuators for 3-DOF micromanipulators in laser phonomicrosurgery," *MESA 2014 - 10th IEEE/ASME Int. Conf. Mechatron. Embed. Syst. Appl. Conf. Proc.*, 2014.

[4] R. Sindrey and G. M. Bone, "Position Tracking Control of a Miniature Water Hydraulic Rotary Actuator," *J. Dyn. Syst. Meas. Control*, vol. 131, no. 6, pp. 1–8, 2009.

[5] M. M Ghazaly, K. Sato, C. A. Aliza, and A. C. Tan, "Force Characterization of a Rotary Motion Electrostatic Actuator Based on Finite Element Method (FEM) Analysis," *Appl. Mech. Mater.*, vol. 761, pp. 233–237, 2015.

[6] M. M Ghazaly and K. Sato, "Characteristic switching of a multilayer thin electrostatic actuator by a driving signal for an ultra-precision motion stage," *Precis. Eng.*, vol. 37, no. 1, pp. 107–116, 2013.

[7] K. Kiyota, T. Kakishima, H. Sugimoto, and A. Chiba, "Comparison of the test result and 3D-FEM analysis at the knee point of a 60 kW SRM for a HEV," *IEEE Trans. Magn.*, vol. 49, no. 5, pp. 2291–2294, 2013.

[8] K. M. Rahman and S. E. Schulz, "Design of high-efficiency and high-torque-density switched reluctance motor for vehicle propulsion," *IEEE Trans. Ind. Appl.*, vol. 38, no. 6, pp. 1500–1507, 2002.

[9] P. T. Hieu, D. Lee, and J. Ahn, "High Speed 2-Phase 4 / 3 Switched Reluctance Motor for Air-blower Application : Design , Analysis , and Experimental Verification," *2015 18th Int. Conf. Electr. Mach. Syst.*, pp. 4–8, 2015.

[10] K. Lu, P. O. Rasmussen, S. J. Watkins, and F. Blaabjerg, "A New Low-Cost Hybrid Switched Reluctance Motor for Adjustable-Speed Pump Applications," *IEEE Trans. Ind. Appl.*, vol. 47, no. 1, pp. 314–321, 2011.

[11] H. Hayashi, K. Nakamura, A. Chiba, T. Fukao, K. Tungpimolrut, and D. G. Dorrell, "Efficiency improvements of switched reluctance motors with high-quality iron steel and enhanced conductor slot fill," *IEEE Trans. Energy Convers.*, vol. 24, no. 4, pp. 819–825, 2009.

[12] I. Yusri, M. M. Ghazaly, E. A. Alandoli, M. F. Rahmat, Z. Abdullah, M. A. M. Ali, and R. Ranom, "Optimization of the Force Characteristic of Rotary Motion Type of Electromagnetic Actuator Based on Finite Element Analysis," *Proc. Mech. Eng. Res. Day 2016*, pp. 1–2, 2016.

[13] P. Rafajdus, A. Peniak, D. Peter, P. Makyš, and L. Szabó, "Optimization of Switched Reluctance Motor Design Procedure for Electrical Vehicles," *2014 Int. Conf. Optim. Electr. Electron. Equip. (OPTIM)*, pp. 397–404, 2014.

[14] K. M. Rahman, B. Fahimi, G. Suresh, A. V. Rajarathnam, and M. Ehsani, "Advantages of switched reluctance motor applications to EV and HEV: design and control issues," *IEEE Trans. Ind. Appl.*, vol. 36, no. 1, pp. 111–121, 2000.

[15] X. Wang, B. Ge, Z. Wu, and F. J. T. E. Ferreira, "A novel bearingless switched reluctance motor," *COMPEL - Int. J. Comput. Math. Electr. Electron. Eng.*, vol. 31, no. 6, pp. 1681–1695, 2012.

[16] M. Takeno, A. Chiba, N. Hoshi, S. Ogasawara, M. Takemoto, and M. A. Rahman, "Test results and torque improvement of the 50-kw switched reluctance motor designed for hybrid electric vehicles," *IEEE Trans. Ind. Appl.*, vol. 48, no. 4, pp. 1327–1334, 2012.

[17] J. M. Stephenson, "Influence of number of poles per phase in switched reluctance motors," *IEE Proc. B Electr. Power Appl.*, vol. 139, no. 4, pp. 307–314, 1992.

[18] K. Suzuki and H. Dohmeki, "Efficiency Comparison of the Switched Reluctance Motor due to the difference in the electromagnetic material," *2014 Int. Symp. Power Electron. Electr. Drives, Autom. Motion*, pp. 417–420, 2014.

[19] Q. Wu, X. He, D. Jin, S. Wu, and T. Zhang, "Parameter design and FEM analysis for 3-phase 6/4 poles switched reluctance motor," *Proc. 30th Chinese Control Conf.*, pp. 3636–3639, 2011.

[20] P. C. Desai, M. Krishnamurthy, N. Schofield, and A. Emadi, "Novel switched reluctance machine configuration with higher number of rotor poles than stator poles: Concept to implementation," *IEEE Trans. Ind. Electron.*, vol. 57, no. 2, pp. 649–659, 2010.

[21] R. Pupadubsin, N. Chayopitak, S. Karukanan, and P. Champa, "Comparison of Winding Arrangements of Three Phase Switched Reluctance Motor under Unipolar Operation," *2012 15th Int. Conf. Electr. Mach. Syst.*, pp. 1–4, 2012.

[22] B. Bilgin, A. Emadi, and M. Krishnamurthy, "Design considerations for switched reluctance machines with a higher number of rotor poles," *IEEE Trans. Ind. Electron.*, vol. 59, no. 10, pp. 3745–3756, 2012.

[23] K. Lu, U. Jakobsen, and P. O. Rasmussen, "Single-phase hybrid switched reluctance motor for low-power low-cost applications," *IEEE Trans. Magn.*, vol. 47, no. 10, pp. 3288–3291, 2011.

[24] J. T. Shi, X. Liu, D. Wu, and Z. Q. Zhu, "Influence of stator and rotor pole arcs on electromagnetic torque of variable flux reluctance machines," *IEEE Trans. Magn.*, vol. 50, no. 11, 2014.

[25] X. Liu and Z. Q. Zhu, "Electromagnetic performance of novel variable flux reluctance machines with DC-field coil in stator," *IEEE Trans. Magn.*, vol. 49, no. 6, pp. 3020–3028, 2013.